

# Colour-Magnitude Diagrams - Astro01

James R. McMurray

*Demonstrator: Dr. Jennifer Hatchell*

(Dated: February 12, 2011)

Colour-magnitude diagrams were produced for the M15 globular cluster and the h+ $\chi$  Persei double open cluster using provided observation data and data reduction methods with the *IRAF* software package. From the use of isochrone data based on theoretical models of stellar evolution, the age of the M15 cluster was estimated to be approximately 13 Gigayears and the age of the h+ $\chi$  Persei double cluster was estimated to be approximately 4 Megayears.

## INTRODUCTION

In this investigation the age of two stellar clusters was estimated through the reduction of provided photometric data, and the production of Hertzsprung-Russell diagrams. The stellar clusters investigated were the globular M15 cluster and the open double cluster of h Persei and  $\chi$  Persei.

## THEORY

### Stellar Luminosity and Effective Temperature

Stars emit continuous radiation in addition to discrete spectral lines from the stimulated emission of photons. The continuous radiation can be effectively modelled by the black body radiation distribution given in Equation (1), in terms of wavelength[1].

$$I_{\lambda}(\lambda, T_s) = \frac{2hc^2}{\lambda^5} \frac{1}{\exp(hc/\lambda kT_s) - 1} \quad (1)$$

Where  $I_{\lambda}$  is the power emitted per unit wavelength per unit area per unit solid angle,  $\lambda$  is the wavelength,  $T_s$  is the effective surface temperature,  $h$  is Planck's constant,  $c$  is the speed of light in a vacuum and  $k$  is Boltzmann's constant.

Note that the presence of absorption lines in the spectrum (characteristic of the elements in the star and our atmosphere) means that it is not truly a black-body.

The peak wavelength of the distribution is related to the temperature by Wien's Law given in Equation (2).

$$T_s \lambda_{\text{peak}} = b \quad (2)$$

where  $T_s$  is the effective surface temperature,  $\lambda_{\text{peak}}$  is the peak wavelength and  $b$  is a constant termed Wien's displacement constant.

The stellar luminosity, the amount of electromagnetic energy radiated per unit time, is related to the effective temperature and stellar radius by the Stefan-Boltzmann equation, given in Equation 3.

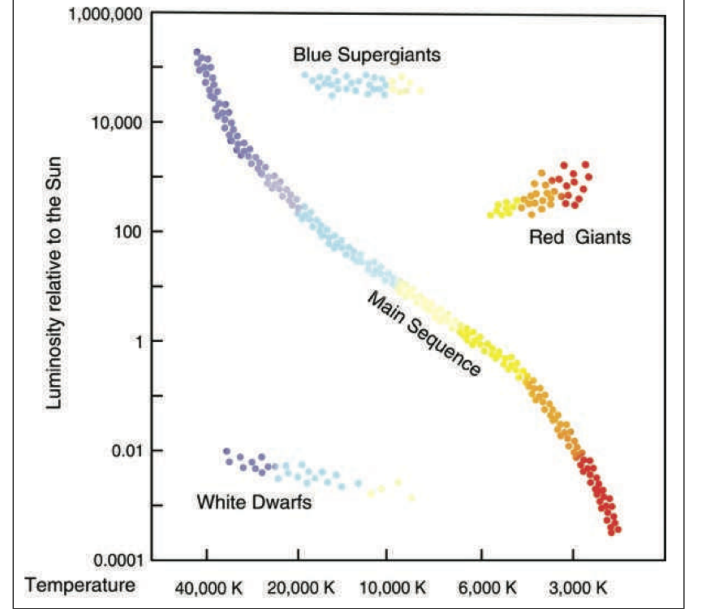


**FIG. 1:** An annotated example of a Hertzsprung-Russell diagram. Adapted from [2].

$$L = 4\pi R^2 \sigma T_s^4 \quad (3)$$

Where  $L$  is the stellar luminosity in Watts,  $R$  is the stellar radius,  $\sigma$  is Stefan's constant and  $T_s$  is the effective surface temperature.

An example of a Hertzsprung-Russell diagram is shown in Figure 1. Note that this is an idealised image that contains every possibility, in the data that is observed there will be a minimum luminosity limit due to the aperture size of the telescope (and so any white dwarfs will not be visible) and there will be many less stars as faint ones cannot be detected. The age is estimated as stars peel off from the main sequence to become red giants.

### Magnitudes and Colours

The flux of an object is the amount of radiation received per unit area per unit time. The magnitude system is used to quantify the flux, relative to a standard

star, for the purposes of comparison[2]. The scale is logarithmic to the base 10, because the response of the human eye is logarithmic. The equation for the apparent magnitude of the star (the magnitude independent of distance) is given in Equation (4).

$$m - m_0 = 2.5 \log_{10}(F_0/F) \quad (4)$$

Where  $m$  is the apparent magnitude,  $m_0$  is the magnitude of the standard star,  $F$  is the flux of the observed star, and  $F_0$  is the flux of the standard star. Note that this equation means that brighter stars have lower numerical apparent magnitudes.

The star Vega is used as the standard star and is defined to have a magnitude of  $m_0 = 0$ , since the flux is well-measured at many wavelengths.

The absolute magnitude takes in to account the distance to the star. The equation for the absolute magnitude is given in Equation (5).

$$M = m - 5 \log_{10}(D_{\text{pc}}) + 5 \quad (5)$$

Where  $M$  is the absolute magnitude,  $m$  is the apparent magnitude and  $D_{\text{pc}}$  is the distance to the object in parsecs.

The absolute magnitude is defined as the magnitude that the object would have if it were at a distance of ten parsecs, and so this removes the effect of variable distance and allows for the direct comparison of the luminosity of different stars.

Magnitudes are measured for a broad range of wavelengths, the difference in magnitudes of an object, between wavelength filters, is known as the colour index.

The colour of a star depends on the peak wavelength of the blackbody radiation, and so from Wien's Law (Equation (2)) depends upon the temperature.

The magnitude relates to the luminosity of the star (the more negative the magnitude is, the brighter the star is), whilst the colour relates to the temperature of the star as described previously, which defines the spectral class of the star (from O, B, A, F, G, K and M, in order of temperature from hot to cool).

An example of a Colour-Magnitude diagram is given in Figure 2. The brighter stars are higher up the graph as a smaller magnitude means a higher luminosity, the hotter stars are on the left of the graph as hotter stars emit a greater proportion of blue light, and so this results in a smaller B-V colour index. This is also true for graphs using the V-R colour index, as hotter stars emit a greater proportion of green light than red light.

Note that the magnitude axis is plotted from positive to negative since negative magnitude values relate to a higher luminosity than positive ones.

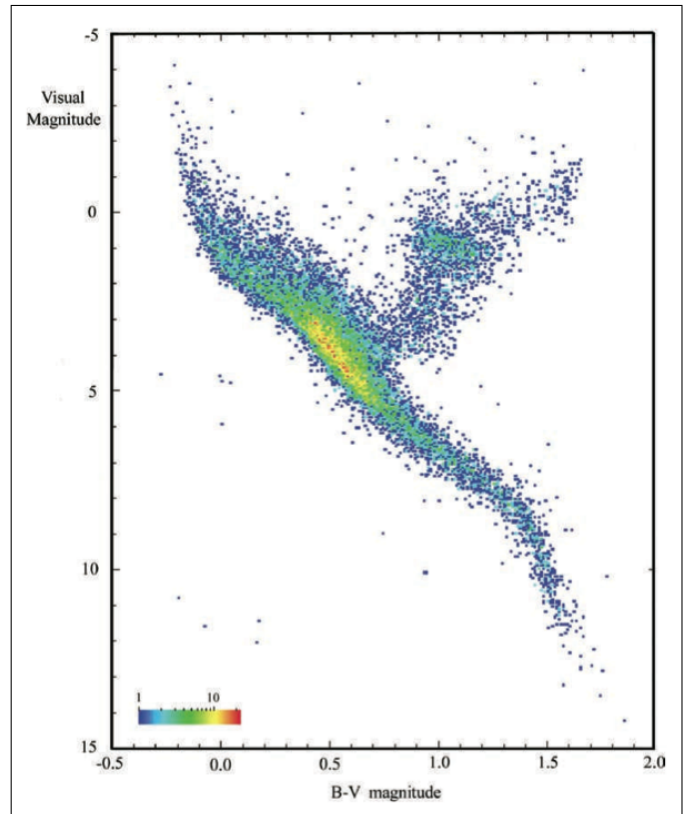


**FIG. 2:** An annotated example of a Colour-Magnitude diagram. Note that this diagram includes all the stars in the local neighbourhood and is not of a specific cluster, this is why it includes all types of stars.

Adapted from [2].

### Stellar Evolution

Stars on the main sequence fuse hydrogen nuclei to produce helium nuclei in the core by the proton-proton chain, this provides the pressure to resist the gravitational attraction which would cause the star to collapse in on itself if unopposed[3]. Eventually the stars deplete all the hydrogen fuel in the core and the fusion stops, this results in the core contracting and the temperature increasing, this increased temperature then makes it possible to fuse helium nuclei together to form carbon nuclei in the triple alpha process, and the stars become red giants.

This increase in temperature and luminosity means that the stars drift off the main sequence on HR diagrams as they become red giants. This turning point can be modelled and used to estimate the age of star clusters, since it is known how long it takes a star of a particular spectral class to reach the end of its main sequence lifetime.

To estimate the age from the colour-magnitude diagrams, isochrones are used, which are predictions of the trend of the colour-magnitude diagram for clusters of a

particular age, based upon theoretical models of stellar evolution.

### Interstellar Reddening

Interstellar reddening is the phenomenon of the dimming and reddening of interstellar light caused by the attenuation from dust clouds[3]. The reddening occurs because blue light is attenuated to a greater extent than redder light.

On colour-magnitude diagrams the interstellar reddening results in the observed stars being shifted down (due to the dimming) and right (due to the reddening) from their intrinsic positions.

### METHOD

The observation data for this investigation was provided. The data was reduced using the *IRAF* software package.

For this data reduction, four calibration images were necessary:

**Flatfield image::** The flatfield image (also known as a “sky flat” when of a blank sky or a “dome flat” when of a uniformly illuminated panel) is an image taken of a source of uniform illumination. This is then used to adjust for the differences between the gain in pixels in the CCD and so normalise the corrected image as they are divided by it. In this case it is advantageous to use the most luminous source possible that does not saturate the CCD pixels, so the relative difference is greatest.

**Dark Frame::** This is an image of a completely dark area (i.e. with the shutter closed) and it is subtracted from the image to compensate for the CCD counts produced by thermal effects.

**Bias Frame::** The bias frame is an image taken with no exposure time, and is subtracted from the image to compensate for the effects of noise produced by the electronics of the CCD.

**Sky Background::** This is an image of an empty sky, taken at the same time as the astronomical images, and is subtracted from the images to correct for the effects of atmospheric light diffusion (including artificial light pollution).

### Data reduction of M15 Images

Some anomalies were present in the sky flat images from dust on the CCD lens and differences in gain between the CCD pixels. The last images in the stack of

sky flats were darker than the first images, for the V filter the first image had a median of 22767 whilst the last image had a median of 15508 and for the R filter the first image had a median of 20946 and the last image had a median of 14297. The dimming was somewhat visible on the images themselves and is likely to be the result of the rapidly darkening sky at twilight in the evening.

The stack of sky flat images for both the R and V filters were combined and then normalised (divided by their median) to make the median of the final flat have a value of 1, so it did not affect the magnitude of the other images when they were divided by the flat. Prior to normalisation the median value of the combined V sky flat was 22787 and the median value of the combined R sky flat was 20957.

A set of six clear images were then chosen from the set of astronomical images for each filter. The other images contained many defects, mostly from blurring caused by atmospheric interference and cloud cover, and streaking caused by the Earth’s rotation during exposure for the images of longer exposure times. All the images used were of 30 seconds exposure time.

The combined sky background images for each filter were then subtracted from the astronomical images, the median value for the visible filter sky background was 165.7 while the median value for the red filter sky background was 185.3. Note that the telescope automatically produces and subtracts the dark frame and bias frame images to account for electronic and thermal effects from the CCD. The astronomical images were then divided by the normalised sky flats to account for the non-uniform response of pixels in the CCD array.

The astronomical images for each filter were then aligned using a reference star in the image to align to. After being shifted by the appropriate distance to align the star on all the images, the images were combined to produce a final image for each of the V and R filters. These images were then aligned with each other so they could be directly compared in the photometry.

### V and R photometry of M15 and h+ $\chi$ Persei

The stars in the images were then selected using the *daofind* function in *IRAF*. For the h+ $\chi$  Persei cluster combined and aligned images were provided. To do this, the Full Width Half Maximum value had to be estimated so that appropriate circles could be fitted to the stars. For the M15 cluster the FWHM value was 3.90 for both filters, for the h+ $\chi$  Persei cluster the FWHM value chosen for the visible filter was 3.88 and for the red filter was 3.46.

The  $\sigma$  value also had to be set to identify the stars, this is the standard deviation required from the background for the element to be considered a star (rather than just background light). A  $\sigma$  value of 1 was used for both

clusters.

After the stars had been identified it was verified that the same stars are located in both the V and R images. The *phot* function was then used to produce a data file containing the positions and magnitudes for all of the stars for both clusters. A star with known magnitude was provided for each cluster, and this was used to produce calibrated apparent magnitudes for the stars by adding the offset to all of the magnitudes. For the h+ $\chi$  Persei cluster the offsets were -3.401 for the V filter and -2.882 for the R filter, for the M15 cluster the offsets were -3.658 for the R filter and -3.35 for the V filter (the signs given such that they were added to the magnitude values).

The distances to each of the clusters were then ob-

tained from known sources, these were 2.3 kpc for the h+ $\chi$  Persei cluster[4] and 10.3 kpc for the M15 cluster[5], and these distances were used to convert the apparent magnitudes to absolute magnitudes.

The V-R colour index for each star was then calculated from the difference in the absolute magnitudes through both filters. The absolute V magnitudes are then used against this V-R colour index to produce a  $M_V$  against V-R colour-magnitude diagram for each cluster.

The isochrones were plotted on the diagrams using isochrone data from *Marigo et al.*[6]. The metallicity value for the M15 cluster was used as  $1.5 \times 10^{-4}$ [7] while the metallicity of the Sun was used for the h+ $\chi$  Persei cluster[8].

## RESULTS

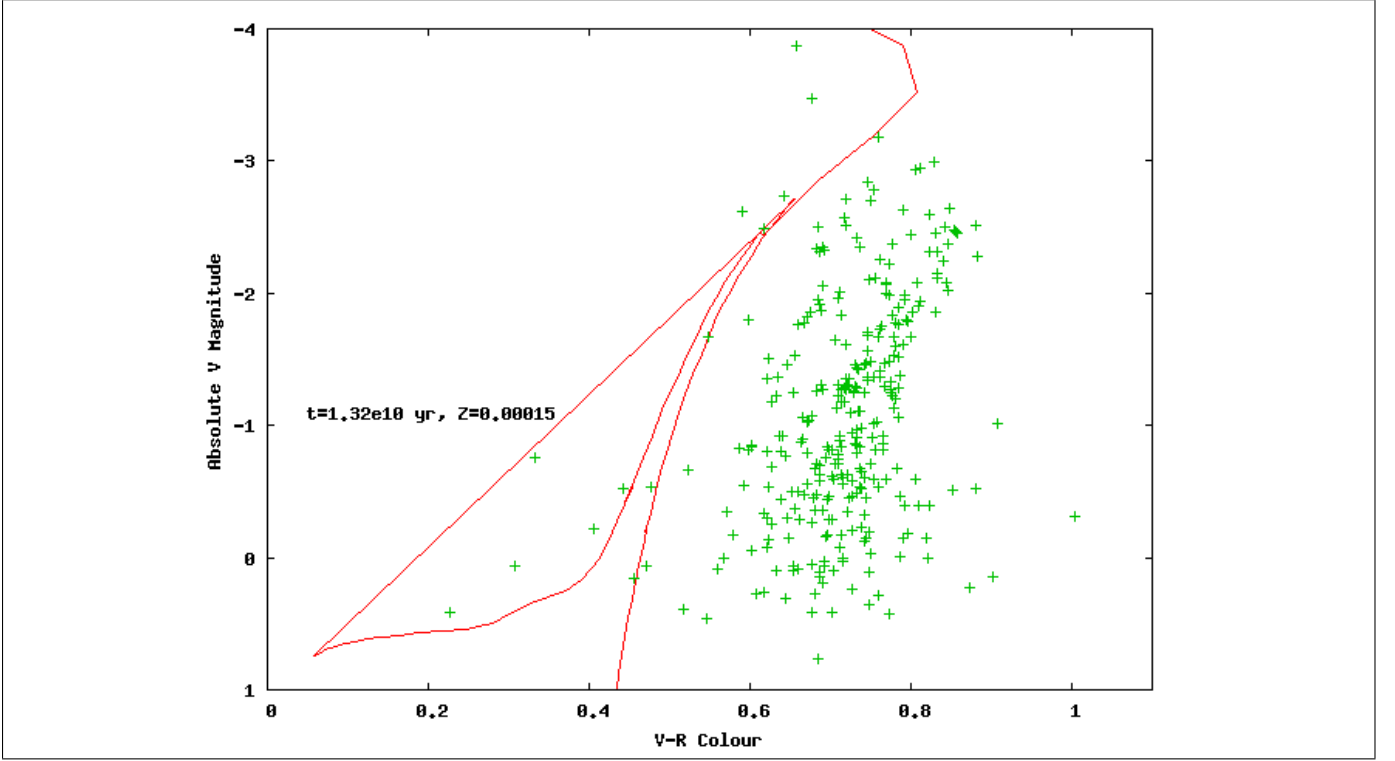


FIG. 3: The colour-magnitude diagram produced for the M15 cluster with the isochrone.

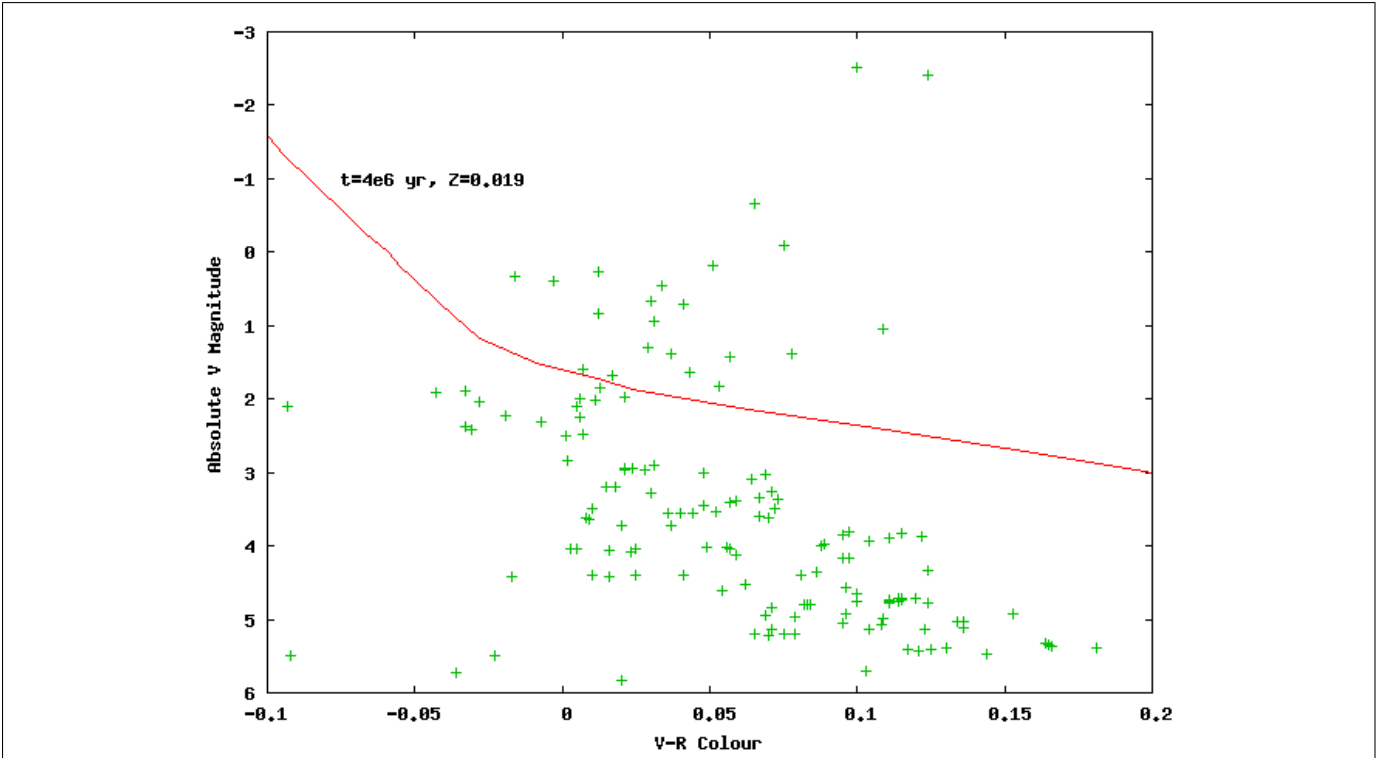


FIG. 4: The colour-magnitude diagram produced for the h Persei and  $\chi$  Persei double cluster with the isochrone overlaid.

## DISCUSSION

The magnitude relates to the luminosity of the stars, where a more negative magnitude relates to a more luminous star. The colour index represents the temperature and stellar classification of the stars, and hotter stars have a smaller colour index.

The  $h+\chi$  Persei cluster is mainly formed of stars lying on the main sequence whereas the M15 cluster has many more red giants. Main sequence stars fuse hydrogen nuclei to produce helium nuclei in the core to and the pressure which resists gravitational collapse. Red giants are formed when the stars exhaust the hydrogen and helium fuel in the core and the increased contraction of the star results in the fusion of helium nuclei in to carbon nuclei via the triple alpha process in the core (note that the red giants may still fuse hydrogen to helium in the shell).

The  $h+\chi$  Persei colour magnitude diagram has very few stars off the main sequence, this suggests it is relatively young compared to the M15 cluster where the red giant branch and the beginning of the horizontal branch are visible. Note that many stars may not be visible due to the luminosity limitations of the telescope used (depending on the aperture size), and so the colour-magnitude diagrams produced have effectively cut off the bottom.

From the isochrones the age for the M15 cluster is estimated to be approximately 13Gyr whilst the age for the  $h+\chi$  cluster is estimated to be approximately 4Myr. This supports the observations from the comparison of the colour-magnitude diagrams that the  $h+\chi$  Persei double cluster is younger than the M15 cluster.

The isochrones do not fit the data perfectly, however this is partly because the isochrones are based upon data using the intrinsic luminosity and colour of the stars, whereas the observation data is affected by interstellar reddening, which results in a shift towards the bottom right.

## CONCLUSIONS

The colour magnitude diagrams were produced from the reduced data for both clusters. From the diagrams and the use of isochrone data, the ages were estimated at approximately 13 Gigayears for the M15 cluster, and approximately 4 Megayears for the  $h+\chi$  Persei double cluster.

- [2] I. Morison, in *Introduction to Astronomy and Cosmology* (Wiley, Chichester, UK, 2008) p. 26, ISBN 978-0-470-03333-3
- [3] M. Inglis, *Astrophysics is easy!* (Springer, 2007) ISBN 978-1-85233-890-9
- [4] C. Siesnick *et al.*, ApJ **576** (2002)
- [5] T. H. B. McNamara and H. Baumgardt, ApJ **602**, 264 (2004)
- [6] Marigo *et al.*, A&A **482**, 883 (2008)
- [7] W. Harris, AJ **112**, 1487 (1996)
- [8] N. G. M. Asplund and A. J. Sauval, Communications in Asteroseismology **147**, 76 (2006)

---

[1] L. Harra and K. Mason, in *Space Science* (Imperial College Press, London, 2004) p. 251, ISBN 1-86094-346-2